Supporting Information

Tetraamino-Driven Hydrogen-Bonding Networks: A Selective Self-Assembly Paradigm for Energetic Materials

Yaxi Wang [a‡], Junliang Liu [a‡], Jinxuan He [b], Xiaoting Ren [b], Lu Hu [a*] and Siping Pang [a*]

[a] School of Materials Science & Engineering, Beijing Institute of Technology, Beijing 100081, China;

[b] National Key Laboratory of Aerospace Chemical Power, Hubei Institute of Aerospace Chemotechnology, Xiangyang, 441003, Hubei, China.

*Corresponding authors. Email: lhu@bit.edu.cn (L. Hu), pangsp@bit.edu.cn (S. Pang)

Contexts

1. Experimental section

Caution! Although we have not experienced any difficulties in preparing and handling these new energetic materials, proper protective precautions must be used. All compounds should be handled with care using the best safety practices.

General Methods: All reagents were obtained from Alfa Aesar or AK Scientific and were used as supplied. A Bruker AVANCE 400 nuclear magnetic resonance spectrometer operating at 400, and 101 MHz was used to collect ^{1}H and ^{13}C spectra, respectively. DMSO-d_6 was employed as solvent and locking solvent. Chemical shifts are given relative to Me_4Si for ^{1}H and ^{13}C spectra. Simultaneous thermal analysis (TG-DSC) was measured by a American-TA-SDT 650 at a scan rate of 5 °C min^{-1}. Densities were determined at room temperature by a Micromeritics AccuPyc 1340 gas pycnometer. IR spectra were recorded on a FT-IR spectrometer (Thermo Nicolet AVATAR 370) as thin films using KBr plates. The impact and friction sensitivities were obtained by using a standard BAM Fall hammer and a BAM friction tester. HRMS data was obtained on a Thermo Fisher-Q Exactive Plus mass spectrometer. XRD data was obtained on a Bruker D8 Advance. Elemental analyses were performed on a Vario Micro cube Elementar Analyser.

5,6-diamino-2,3-pyrazinedicarbonitrile was synthesized by reported literatures (Reference 22 in article).

2,5,6,9-Tetramino-Pyrazino[2,3-*d*]pyridazine (TPP)

5,6-diamino-2,3-pyrazinedicarbonitrile (0.80 g, 5.0 mmol) was mixed with isopropyl alcohol (50.0 mL). Then, hydrazine hydrate (98.0 wt%, 0.75 mL, 15.0 mmol) was added. The solution is heated to 80 °C with stirring at reflux for 16 h. The precipitate was collected by filtration and purified by washing with H_2O to give **TPP** as a reddish-brown solid (0.52 g, 53.6%). ^{1}H NMR ([D_6]DMSO, 400 MHz): δ=7.09 (s, 4H), 5.19 (s, 4H) ppm; ^{13}C NMR ([D_6]DMSO, 101 MHz): δ=151.69, 147.27, 123.51 ppm; IR (KBr pellet): 3427, 3363, 3343, 3305, 3253, 3190, 2830, 1677, 1649, 1594, 1509, 1452, 1384, 1352, 1326, 774, 750, 683, 637, 620, 608, 552, 534, 518, 510, 504, 496, 486 cm^{-1}; HRMS (ESI) m/z

calculated for $[C_6H_8N_8\text{-}H]^-$ 191.0794, found 191.0791; elemental analysis ($C_6H_8N_8$, 192.19): calcd C 37.50, H 4.20, N 58.31; found C 37.46, H 4.21, N 58.14.

2,5,6,9-tetramino-pyrazino[2,3-*d*]pyridazine-1-ium-hydrochloride (TPP-HCl)

To a powder of **TPP** (0.19 g, 1.0 mmol) was added hydrochloric acid (37.0 wt%, 10.0 mL) in portions. The mixture became a yellow clarified solution, and then the temperature was raised to reflux and stirred for 3 h. The precipitation was filtered, and the filtrate was collected and vacuum dried to obtain the yellow crystal **TPP-HCl** (0.140 g, 60.7%). ^{1}H NMR ([D_6]DMSO, 400 MHz): δ=7.99 (s, 4H), 7.00 (s, 4H) ppm; ^{13}C NMR ([D_6]DMSO, 101 MHz): δ=150.16, 148.40, 125.44ppm; IR (KBr pellet): 3427, 3404, 2830, 2718, 1631, 1593, 1509, 1384, 1353, 773, 680, 653, 622, 601, 571, 547, 517, 497, 477, 464, 456, 449, 436, 428, 419, 401 cm^{-1}; HRMS (ESI) m/z calculated for $[C_6H_8ClN_8\text{-}H]^-$ 227.0560, found 227.0561; elemental analysis ($C_6H_9ClN_8$, 228.64): calcd C 31.52, H 3.97, N 49.01; found C 31.47, H 4.02, N 48.93.

2,5,6,9-tetramino-pyrazino[2,3-*d*]pyridazine-1-ium-perchlorate (TPP-$HClO_4$)

To a suspension of **TPP** (2.0 mmol, 0.384 g) in water (10.0 mL) was added perchloric acid (70 wt%, 0.2 mL) in portions. The mixture became a brown clarified solution, and then the solution was stirred for another 2 h at 80 °C and filtered to obtain the brown-yellow solid **TPP-$HClO_4$** (0.165 g, 56.2%). ^{1}H NMR ([D_6]DMSO, 400 MHz): δ=7.63 (s, 4H), 6.79 (s, 4H) ppm; ^{13}C NMR ([D_6]DMSO, 101 MHz): 123.84, 127.39, 147.71,148.96,150.56 ppm; IR (KBr pellet): 3447, 3370, 2831, 2716, 1631, 1596, 1355, 1143, 1115, 1079, 775, 682, 625, 579, 555, 537, 515, 499, 491, 471, 458, 451, 439, 425, 417, 404 cm^{-1}; HRMS (ESI) m/z calculated for $[C_6H_9ClN_8O_4\text{-}H]^-$ 291.0357, found 291.0360; elemental analysis ($C_6H_9ClN_8O_4$, 292.64): calcd C 24.63, H 3.10, N 38.29; found C 24.57, H 3.16, N 38.17.

2. X-ray Crystallography

Crystal Structure Analysis: The X-ray diffraction data were measured on Bruker D8 Venture PHOTON II CPAD diffractometer equipped with a MoKα INCOATEC ImuS micro-focus source (λ=1.54178 Å). Indexing was performed using Apex3.[1] Data

integration and reduction were performed using Saint.[2] Absorption correction was performed by multi-scan method implemented in SADABS.[3] Space groups were determined using XPREP implemented in APEX3.[4] The structure was solved using SHELXT and refined using SHELXL-2018 (full-matrix least-squares on F^2) within OLEX2 interface program.[5,6] All non-hydrogen atoms were refined anisotropically. All hydrogen atoms were placed in geometrically calculated positions and were included in the refinement process using riding models with isotropic thermal parameters.

A variety of solvent systems have been tried during crystal growth. The neutral compound TTP could not be crystallized in DMSO, DMF and other solvents, and finally TPP-H_2O was obtained in a mixture of DMSO and H_2O. Crystals of **TPP-HCl** and **TPP-$HClO_4$** were successfully grown in different solvent systems, yet their unit cell parameters are nearly identical. These results demonstrate the same selective encapsulation in self-assembly.

Table S1. Single Crystal Growth Methods.

Compounds	solvent	whether to obtain single crystal
TPP-H_2O	DMSO	NO
	DMF	NO
	H_2O	NO
	DMF+H_2O	NO
	DMSO+H_2O	**YES**
TPP-HCl	MeCN	NO
	MeOH	**YES**
	H_2O	**YES**
TPP-$HClO_4$	H_2O	NO
	MeCN	**YES**
	MeOH	**YES**

Table S2. Cell parameters of **TPP-HCl** and **TPP-$HClO_4$** in different solvent systems.

Compounds	solvent	Cell parameters		
		a (Å)	b (Å)	c (Å)
TPP-HCl	MeOH	27.62	3.90	21.68
	H_2O	27.56	3.82	21.72
TPP-$HClO_4$	MeCN	6.85	15.85	9.86
	MeOH	6.98	15.92	9.79

Crystal data and refinement conditions are shown in **Table S3**, and the crystal structures are shown in **Figure S1-S3**.

Table S3. Crystallographic Data.

	TPP-H_2O	**TPP-HCl**	**TPP-$HClO_4$**
CCDC No.	2433343	2433345	2433344
Formula	$C_6H_{10}N_8O$	$C_6H_9ClN_8$	$C_6H_9ClN_8O_4$
$D_{calc.}$/ g · cm^{-3}	1.666	1.691	1.823
μ/mm^{-1}	0.126	0.405	0.390
Formula Weight	210.22	228.66	292.66
Color	yellow	yellow	yellow
Shape	acicular	acicular	acicular
F(000)	440.0	944.0	600.0
Size/mm^3	0.12×0.06×0.04	0.11×0.06×0.04	0.11×0.04×0.02
T/K	100	100	100
Crystal System	monoclinic	monoclinic	Monoclinic
Space Group	$P2_1/c$	C2/c	$P2_1/n$
a/Å	3.6169(6)	27.527(4)	6.8415(7)
b/Å	19.782(3)	3.8158(5)	15.8632(13)
c/Å	11.752(2)	21.717(3)	9.8345(9)
α/°	90	90	90
β/°	94.717(7)	128.059(4)	92.574(3)
γ/°	90	90	90
V/$Å^3$	838.0(3)	1796.1(4)	1066.24(17)
Z	4	8	4
Radiation type	MoKα	MoKα	MoKα
$2Θ_{min}$/°	4.042	3.84	4.876
$2Θ_{max}$/°	52.77	52.87	52.874
Index ranges	-4≤h≤4, -24≤k≤24, -14≤l≤14	-34≤h≤34, -4≤k≤4, -27≤l≤26	-8≤h≤8, -19≤k≤19, -12≤l≤12
Measured Refl's.	6993	7169	8855
Ind't Refl's	1725	1849	2203
R_{int}	0.0976	0.0988	0.1022
Parameters	176	156	208
Restraints	10	99	8
Largest Peak	0.23	0.54	0.57
Deepest Hole	-0.34	-0.60	-0.69
GooF	1.049	1.052	1.021
wR_2 (all data)	0.1634	0.1627	0.1630
wR_2	0.1301	0.1430	0.1425
R_1 (all data)	0.1288	0.0856	0.0904
R_1	0.0626	0.0589	0.0608

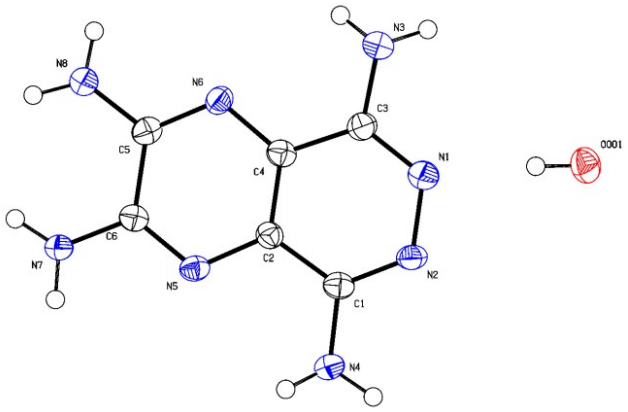

Figure S1. Single-crystal X-ray structure of **TPP-H_2O** (50% probability level).

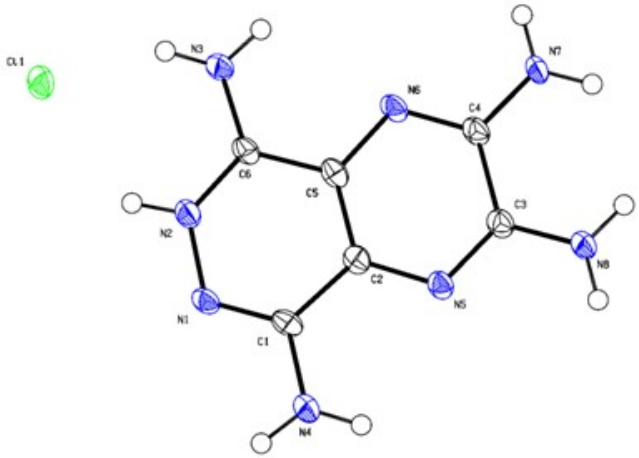

Figure S2. Single-crystal X-ray structure of **TPP-HCl** (50% probability level).

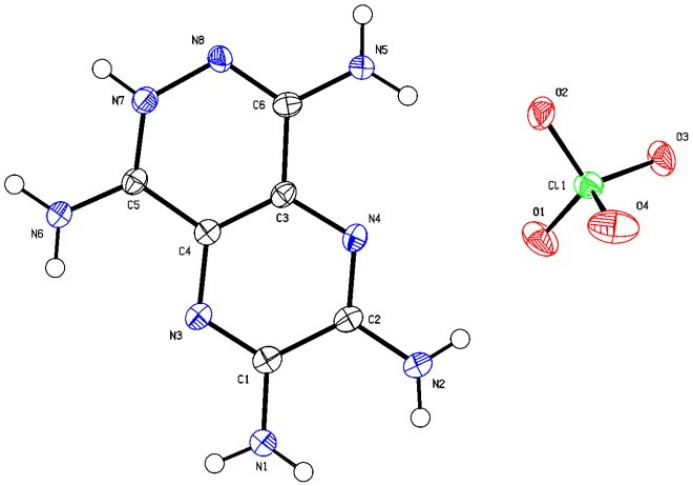

Figure S3. Single-crystal X-ray structure of **TPP-$HClO_4$** (50% probability level).

3. Theoretical calculations

Calculations: The calculations of the heats of formation were carried out using Gaussian 09 (Revision D.01) suite of programs.[7] All the compounds were determined using isodesmic reactions (Fig. S3). The geometric optimization and frequency analyses of the structures were calculated using B3LYP/6-31+G** level. The gas phase enthalpy of formation was computed and the enthalpy of reaction was obtained by combining the MP2/6-311++G** energy difference for the reactions, the scaled zero-point energy (ZPE), values of thermal correction (HT), and other thermal factors. All the optimized structures were characterized to be true local energy minima on the potential energy surface without imaginary frequencies.[7]

The isodesmic reactions for **TPP-HClO$_4$** and energetic anions all follow by the actual crystal structure. The isodesmic reaction (partner = benzene) is shown in **Figure S4**. According to the HOF results in **Table S4**, the HOF of **TPP-HClO$_4$** is 182.2 kJ mol^{-1}.

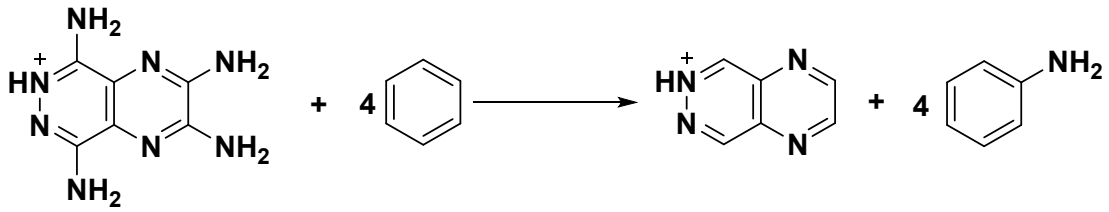

Figure S4. Isodesmic reaction for **TPP-HClO$_4$**.

Table S4. The HOF calculated results of **TPP-HClO$_4$**.

Compound	ΔH_L(KJ·mol^{-1})	$\Delta H_{fcation}$(KJ·mol^{-1})	ΔH_{fanion}(KJ·mol^{-1})	ΔH_f^{298}(KJ·mol^{-1})
TTP-HClO$_4$	469.92691	929.69118	896.39553	182.18661

4. NMR, HRMS data and TG-DSC curves

The NMR, HRMS and TG-DSC curves are shown below. The neutral compound TPP exhibited no discernible endothermic and exothermic phenomena within the tested temperature range (40-450 °C). The thermal decomposition temperatures of **TPP-HCl** and **TPP-$HClO_4$** are 171 and 344 °C, respectively.

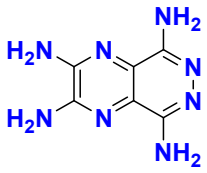

TPP

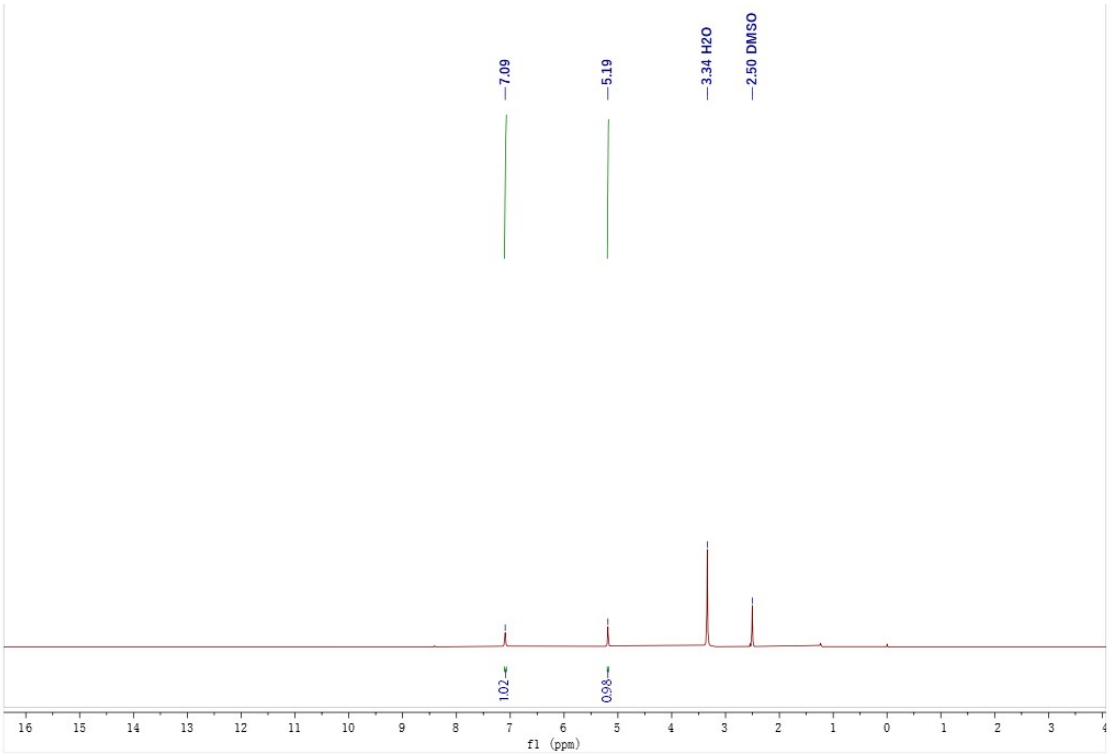

Figure S5. ^{1}H-NMR spectrum of **TPP** in d_6-DMSO.

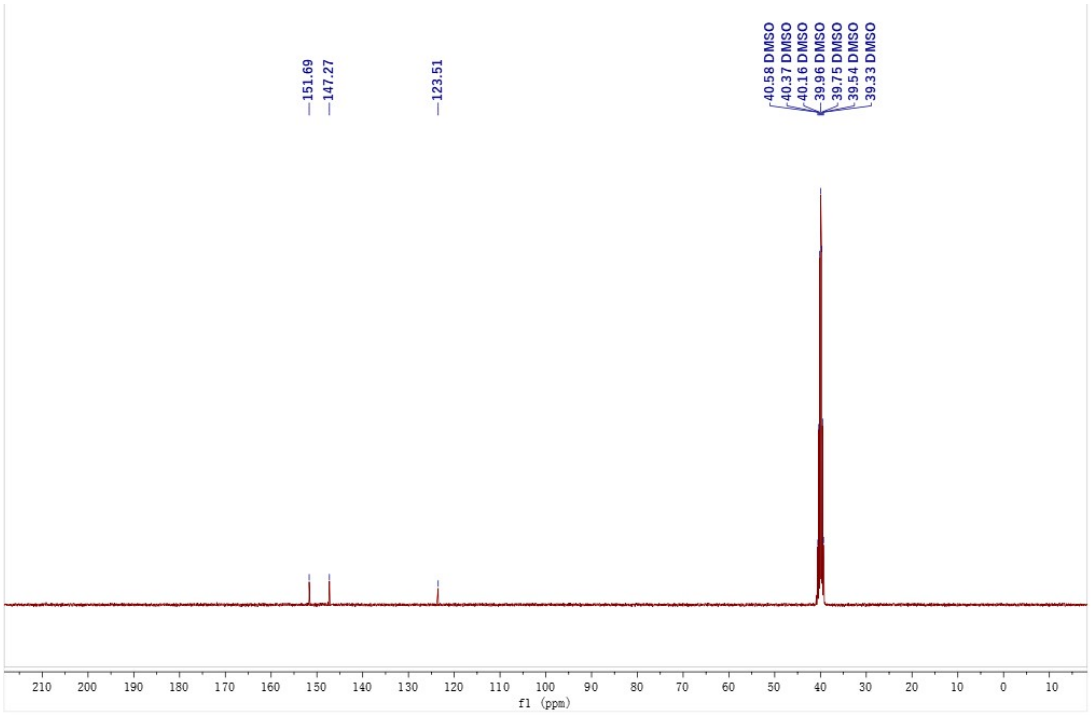

Figure S6. ^{13}C-NMR spectrum of **TPP** in d_6-DMSO.

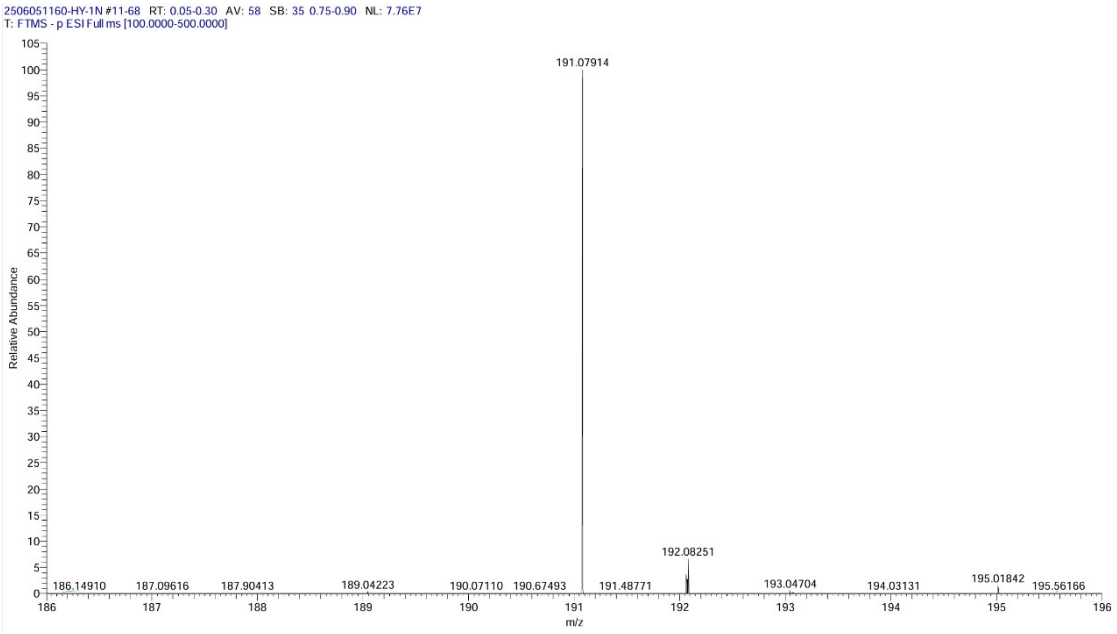

Figure S7. High-resolution mass spectrum data of **TPP**.

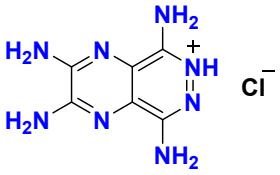

TPP-HCl

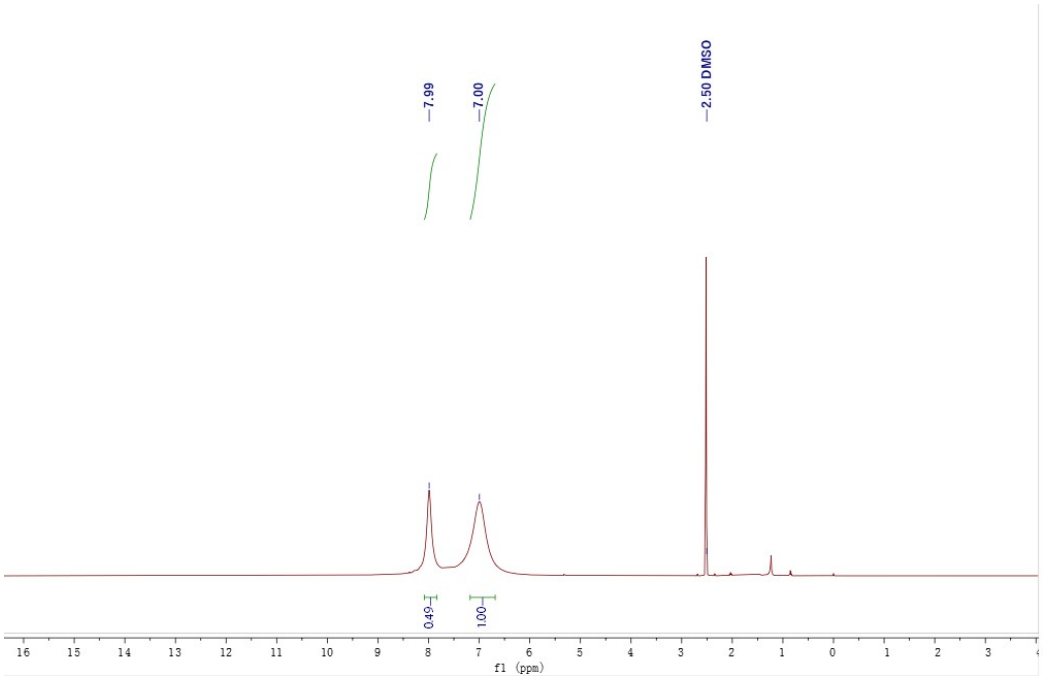

Figure S8. ^{1}H-NMR spectrum of **TPP-HCl** in d_6-DMSO.

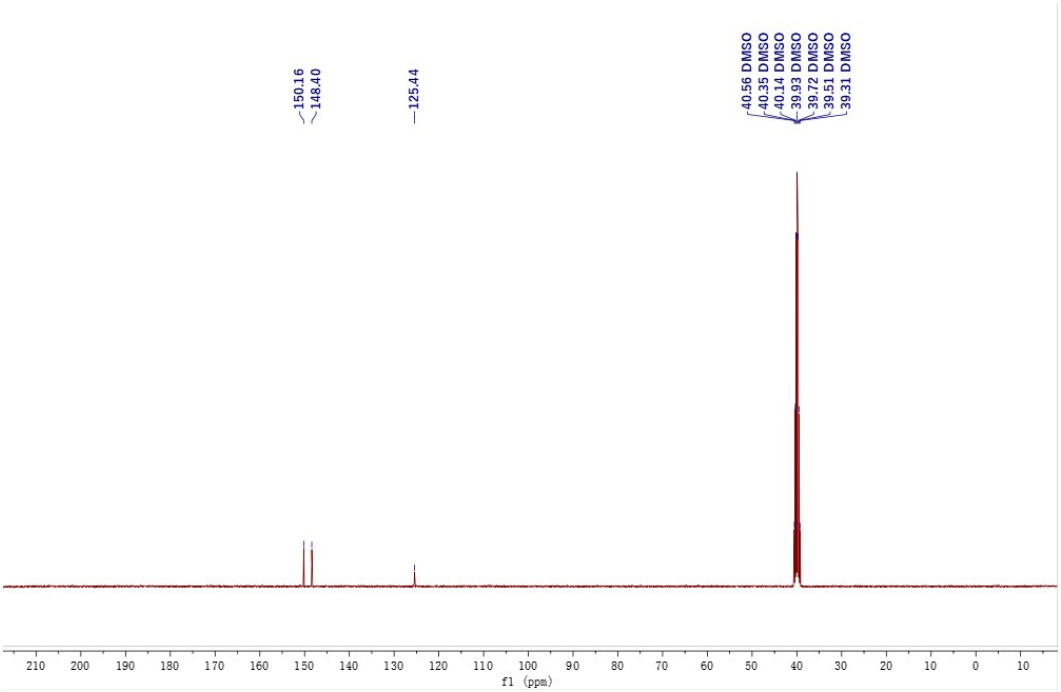

Figure S9. ^{13}C-NMR spectrum of **TPP-HCl** in d_6-DMSO.

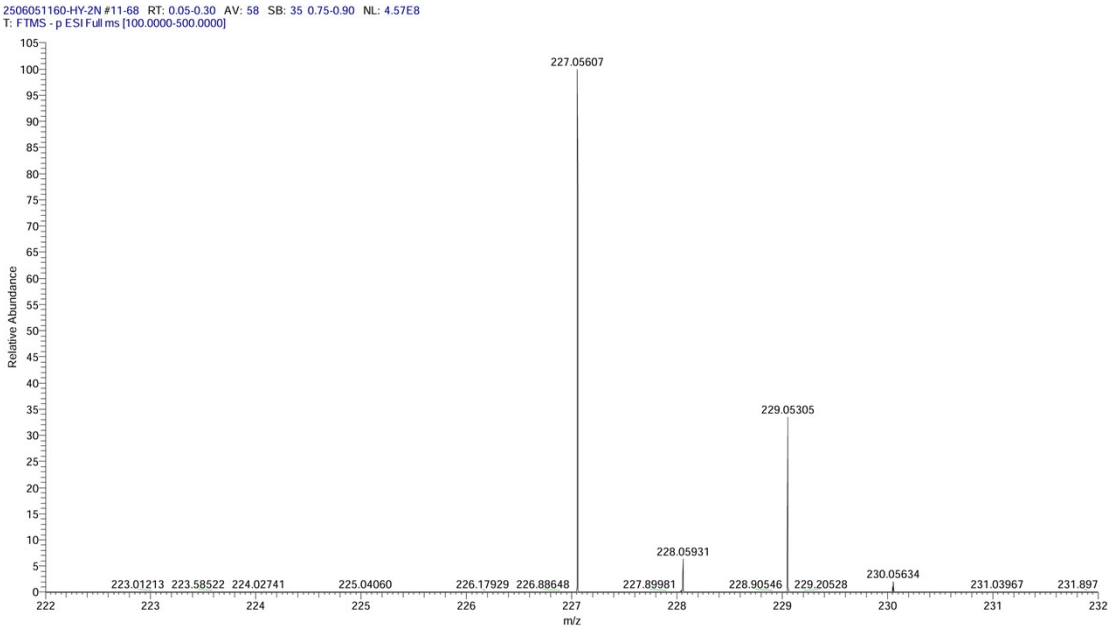

Figure S10. High-resolution mass spectrum data of **TPP-HCl**.

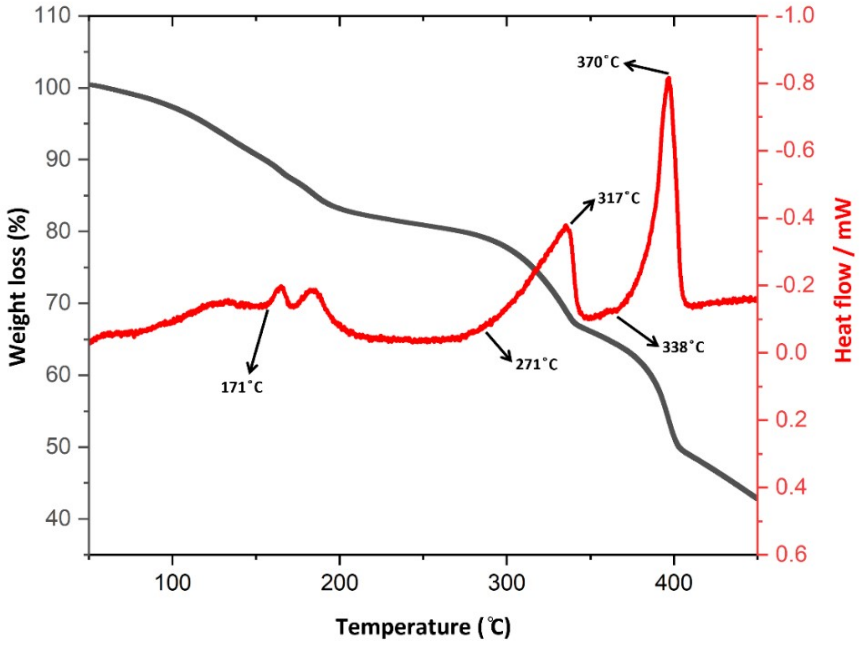

Figure S11. TG-DSC curve of **TPP-HCl** at 5 ℃ min^{-1}.

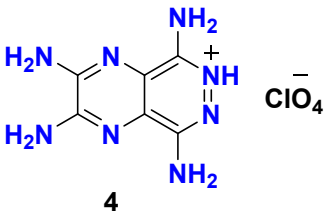

4

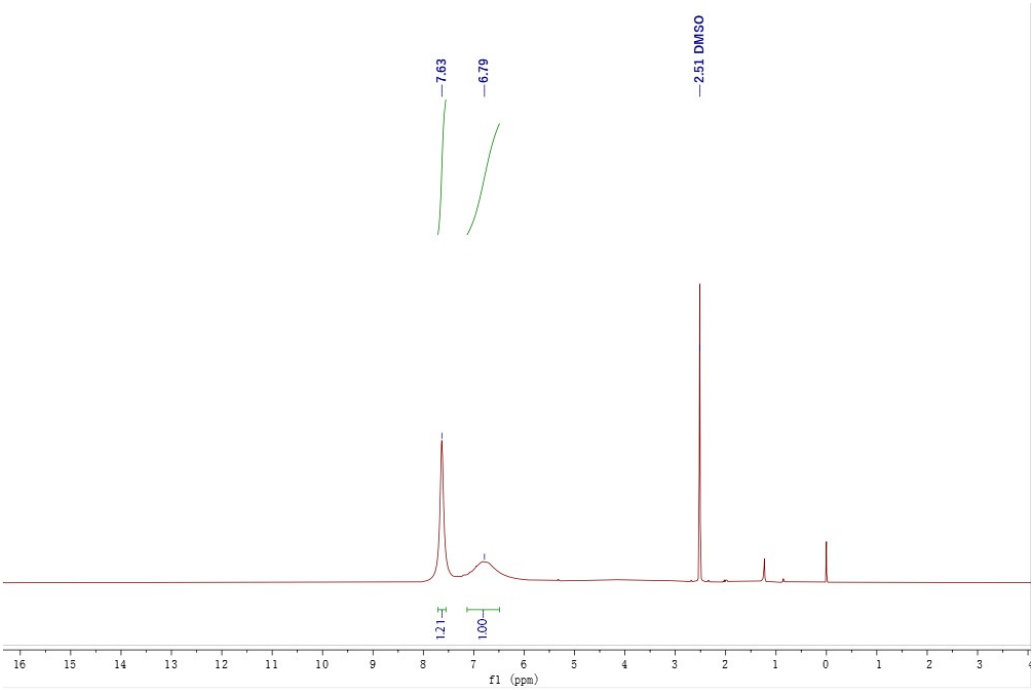

Figure S12. ^{1}H-NMR spectrum of **TPP-HClO$_4$** in d_6-DMSO.

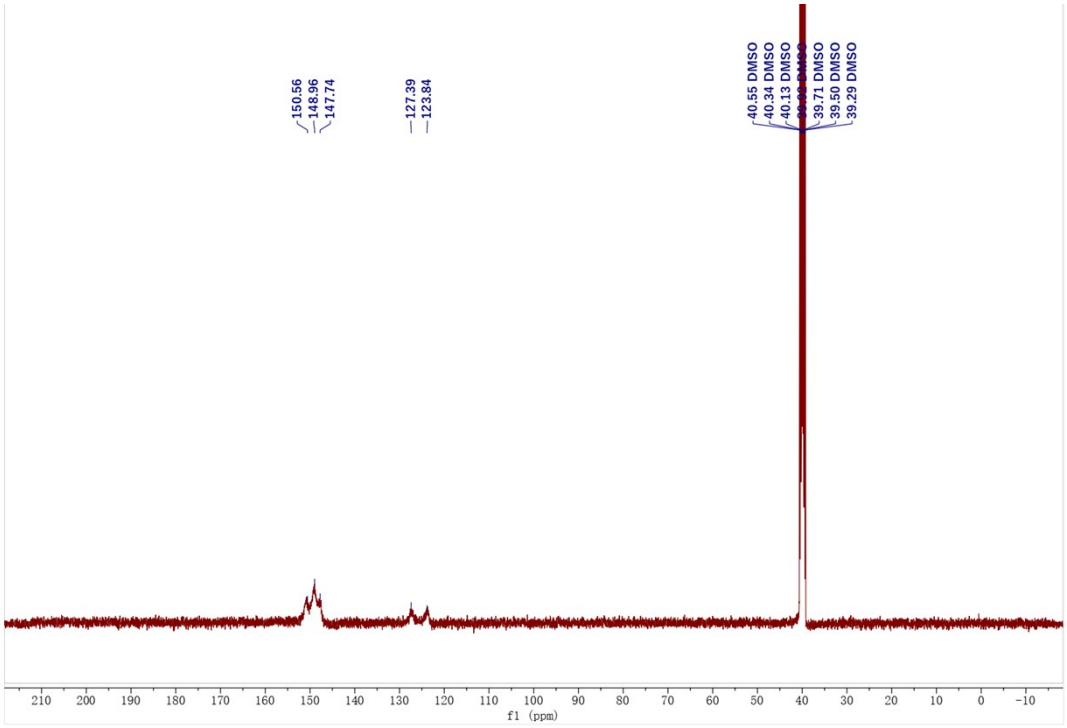

Figure S13. ^{13}C-NMR spectrum of **TPP-HClO$_4$** in d_6-DMSO.

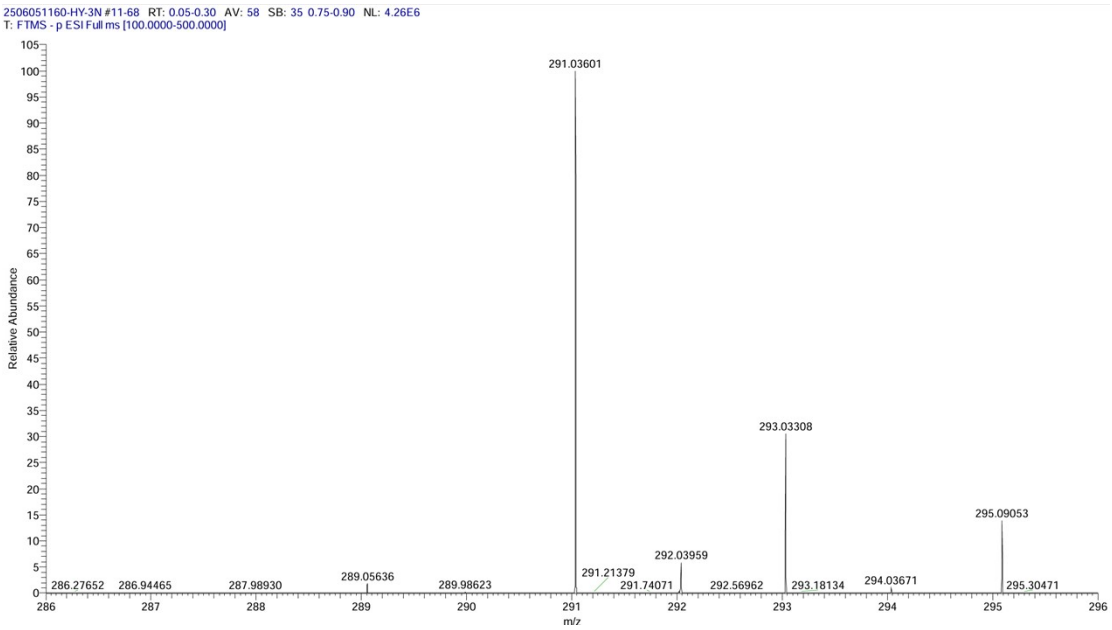

Figure S14. HRMS data of **TPP-HClO$_4$**.

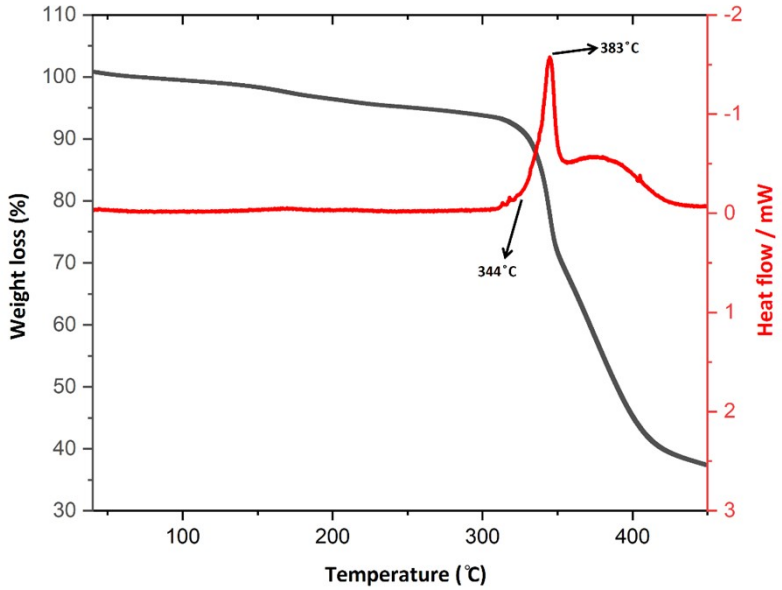

Figure S15. TG-DSC curve of **TPP-HClO$_4$** at 5 ℃ min^{-1}.

5. X-ray diffraction (XRD) patterns

Variable temperature powder X-ray diffraction (VT-PXRD) can further demonstrate that the material maintains crystalline state. Given the potential safety hazards associated with energetic compounds and the risk of corrosive degradation to instrument components from acidic gases released by halogen-containing samples (**TPP-HCl** and **TPP-$HClO_4$**) at elevated temperatures, the upper temperature limit for all VT-PXRD measurements was set up to 100°C. Furthermore, due to the poor thermal stability of **TPP-HCl** observed in TG-DSC analysis, VT-PXRD characterization was restricted to ambient temperature as a safety precaution. The results indicate that the crystals of **TPP-H_2O** and **TPP-$HClO_4$** exhibit excellent stability within the specified temperature range (25, 50, 75 and 100 °C).

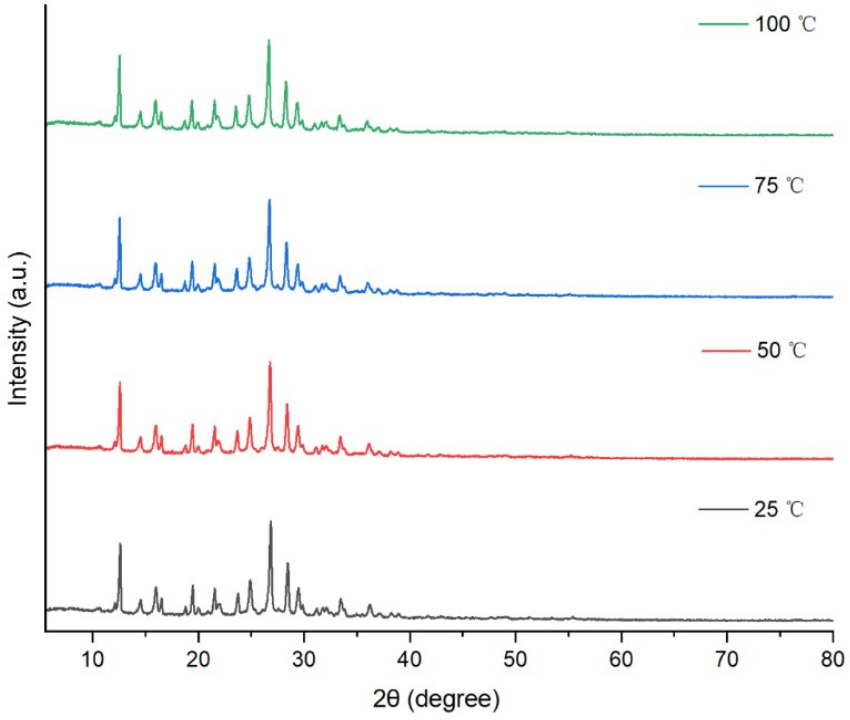

Figure S16. VT-PXRD patterns of **TPP-H_2O**.

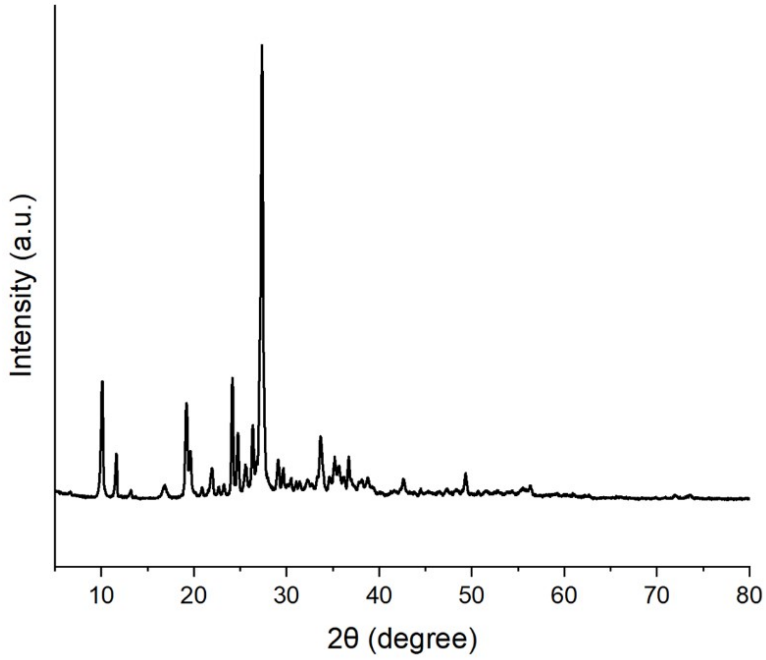

Figure S17. PXRD pattern of **TPP-HCl**.

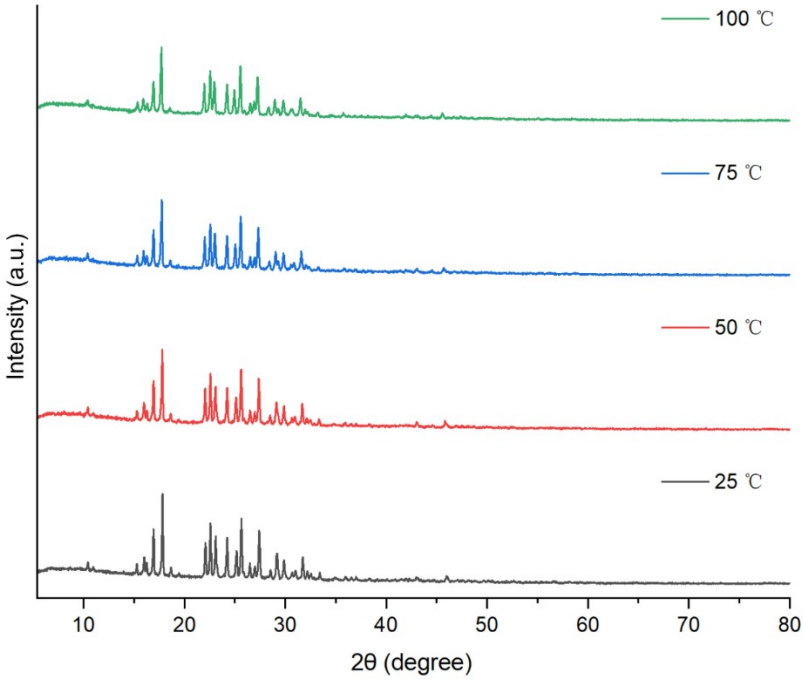

Figure S18. VT-PXRD patterns of **TPP-$HClO_4$**.

References

(1) Bruker (2018). APEX3 (Version 2017.3). Bruker AXS Inc., Madison, Wisconsin, USA.

(2) Bruker (2018) SAINT V8.35A. Data Reduction Software.

(3) Sheldrick, G. M. (1996). SADABS. Program for Empirical Absorption Correction. University of Gottingen, Germany.

(4) Sheldrick, G. M. *Acta Cryst*., 2015, **A71**, 3-8.

(5) Sheldrick, G.M. *Acta Cryst*., 1990, **A46**, 467-473.

(6) Sheldrick, G. M. *Acta Cryst*., 2008, **A64**, 112-122.

(7) Frisch, M. J.; Trucks, G. W.; Schlegel, H. B.; Scuseria, G. E.; Robb, M. A.; Cheeseman, J. R.; Montgomery, J. A.; Vreven, T.; Kudin, K. N.; Burant, J. C.; Millam, J. M.; Iyengar, S. S.; Tomasi, J.; Barone, V.; Mennucci, B.; Cossi, M.; Scalmani, G.; Rega, N.; Petersson, G. A.; Nakatsuji, H.; Hada, M.; Ehara, M.; Toyota, K.; Fukuda, R.; Hasegawa, J.; Ishida, M.; Nakajima, T.; Honda, Y.; Kitao, O.; Nakai, H.; Klene, M.; Li, X.; Knox, J. E.; Hratchian, H. P.; Cross, J. B.; Bakken, V.; Adamo, C.; Jaramillo, J.; Gomperts, R.; Stratmann, R. E.; Yazyev, O.; Austin, A. J.; Cammi, R.; Pomelli, C.; Ochterski, J. W.; Ayala, P. Y.; Morokuma, K.; Voth, G. A.; Salvador, P.; Dannenberg, J. J.; Zakrzewski, V. G.; Dapprich, S.; Daniels, A. D.; Strain, M. C.; Farkas, O.; Malick, D. K.; Rabuck, A. D.; Raghavachari, K.; Foresman, J. B.; Ortiz, J. V.; Cui, Q.; Baboul, A. G.; Clifford, S.; Cioslowski, J.; Stefanov, B. B.; Liu, G.; Liashenko, A.; Piskorz, P.; Komaromi, I.; Martin, R. L.; Fox, D. J.; Keith, T.; Al-Laham, M. A.; Peng, C. Y.; Nanayakkara, A.; Challacombe, M.; Gill, P. M. W.; Johnson, B.; Chen, W.; Wong, M. W.; Gonzalez, C.; Pople, J. A, Gaussian 09, revision D.01; Gaussian, Inc.: Wallingford, CT, 2009.